DOI: 10.1002/zaac.200900265

2-Organoselenomethyl-*1H*-benzimidazole Complexes of Copper(II) and Copper(I)

Markus Leboschka,[a] Monika Sieger,[a] Biprajit Sarkar,[a] Jürgen Heck,[a] Mark Niemeyer,[b] Denis Bubrin,[a] Falk Lissner,[a] Thomas Schleid,[a] Stanislav Záliš,[c] Cheng-Yong Su,[d] and Wolfgang Kaim*[a]

Dedicated to Professor Martin Jansen on the Occasion of His 65th Birthday

Keywords: Coordination modes; Copper; Imidazole ligands; Selenoether ligands; X-ray diffraction

Abstract. Structurally characterized 2-methylselenomethyl-*1H*-benzimidazole (msbi) is shown to form complexes in 2:1 ratio with copper(II). Whereas the central cation $[Cu(msbi)_2Cl]^+$ = $\mathbf{1}^+$ in $[Cu(msbi)_2Cl]Cl\cdot 2MeOH$ crystallizes in an approximately mixed square-pyramidal/trigonal-bipyramidal structure (τ = 0.52) with the second and third row atoms chlorine and selenium in the equatorial plane, the related $[Cu(msbi)_2(MeOH)](BF_4)_2$ = $[\mathbf{2}](BF_4)_2$ exhibits a closer to square-pyramidal arrangement with τ = 0.36 for that complex dication $\mathbf{2}^{2+}$. In both cases, the Cu–N bonds are short at about 1.94 Å, whereas the Cu–Se distances vary between 2.62 Å for $\mathbf{1}^+$ and ca. 2.54 Å for $\mathbf{2}^{2+}$. Slight differences between the Jahn–Teller influenced species $\mathbf{1}^+$ and $\mathbf{2}^{2+}$ are also apparent from absorption and EPR spectra. Since copper(I) complexes of msbi suitable for crystal structure analysis could not be obtained, the related 1-methyl-2-phenylselenomethyl-*1H*-benzimidazole (mpsbi) was prepared and used to obtain $[Cu(mpsbi)_2](X)$ = $[\mathbf{3}](X)$ (X = BF_4 or PF_6). The copper(I) ion in the corresponding cation $\mathbf{3}^+$ shows a DFT-reproduced distorted tetrahedral configuration with an $N–Cu^{I}–N$ angle at 146.7(3)°, less straightened than the ca. 170° in similar Cu^{I} complexes with thioether-*1H*-benzimidazole ligands. A copper(I) compound $[Cu(psbi)_2][Cu(psbi)(psbi-H^+)](PF_6)$ = $[\mathbf{4}][\mathbf{4'}](PF_6)$ with another related ligand, 2-phenylselenomethyl-*1H*-benzimidazole (psbi), was crystallized in partially benzimidazole-deprotonated acetonitrile solvate form, showing short Cu–N bonds of 1.898(5) Å, an $N–Cu^{I}–N$ angle of 157.5(3)°, a Se···Se interaction at 3.6237(3) Å, and a very small Se–Cu–Se angle of 78.23(4)°. The different responses resulting from thioether and selenoether coordination to copper in the complexes at hand are being discussed.

Introduction

Organoselenium ligands are being increasingly used in coordination chemistry [1, 2] due to the biological function of this chalcogen [3, 4]. Whereas the main focus has been on the important biological roles of the easily deprotonated selenocysteine, the "21st essential amino acid" [4], selenomethionine [5] and related selenoethers have been used as probes for NMR spectroscopic and X-ray crystallographic studies of biomolecules [5]. Following our work on copper(I) and copper(II) complexes of mixed imine-N and thioether-S chelate ligands such as 1-methyl-2-(methylthiomethyl)-*1H*-benzimidazole (mmb) [6–8], we have now extended this approach to related imine-N/selenoether-Se ligands.

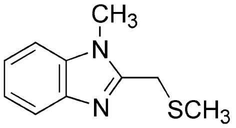

mmb

The mmb and related ligands have not only allowed us to observe [9] the biochemically relevant [10] valence-tautomer equilibrium [Equation (1)] outside of an enzyme [6], it also displayed a remarkable propensity to allow for facile $Cu^{I/II}$ transitions [6–11] because of uncommon coordination arrangements such as illustrated by a "see-saw" configuration [12] around the metal in $[Cu(mmb)_2]^+$ with its 2+2 coordination arrangement (see Figure 8 below) [6].

$$(L)Cu^{I}(Q^{\cdot-}) \rightleftarrows (L)Cu^{II}(Q^{2-}) \qquad (1)$$

(spin on Q)   (spin on copper)

---

* Prof. Dr. W. Kaim
Fax: +49-711-685-64165
E-Mail: kaim@iac.uni-stuttgart.de
[a] Institut für Anorganische Chemie
Universität Stuttgart
Pfaffenwaldring 55
70550 Stuttgart, Germany
[b] Institut für Anorganische und Analytische Chemie
Universität Mainz
Duesbergweg 10–14
55128 Mainz, Germany
[c] J. Heyrovský Institute of Physical Chemistry, v.v.i.
Academy of Sciences of the Czech Republic
Dolejškova 3
18223 Prague, Czech Republic
[d] School of Chemistry and Chemical Engineering
Sun Yat-Sen University
Guangzhou, 510275, P. R. China

In addition to the variation in the “minimal modeling” of certain biochemical functions, molecular copper complexes of sulfur and selenium containing ligands [2] are also of interest as potential precursor components for obtaining copper/indium/gallium/selenide or -sulfide (CIGS) photovoltaic materials $CuMSe_2$ (M = In, Ga) [13].

The coordination of thioether and selenoether functions to transition metals has been reviewed and discussed with respect to the π acceptor influence [1b, 14], whereas recent results of methionine-rich copper(I) metalloproteins with regulatory and other functions [15] also stimulate studies in the field. Following the high-resolution protein structure analysis [16] of the monoxygenase enzyme PHM in the presence of bound dioxygen there have been several studies reported on mixed imidazole-thioether model ligands and their copper complexes [17].

Using the previously [8a] introduced 2-methylselenomethyl-*1H*-benzimidazole (msbi) ligand herein we report results from studies of the copper(I) and copper(II) coordination chemistry of that ligand.

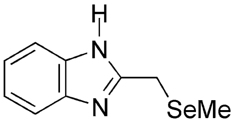

msbi

The inability to obtain a copper(I) complex of msbi suitable for crystal structure analysis prompted us to modify the 2-selenoether-*1H*-benzimidazole chelate system. A structurally characterized copper(I) complex of the new 1-methyl-2-phenylselenomethyl-*1H*-benzimidazole (mpsbi) without the potential for N–H hydrogen bonding was thus obtained and its configuration was confirmed by DFT calculation.

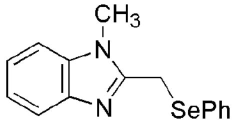

mpsbi

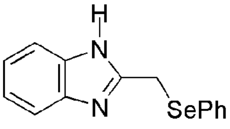

psbi

Another copper(I) complex ion $[Cu(psbi)_2]^+$ was obtained from the previously described [8b] ligand 2-phenylselenomethyl-*1H*-benzimidazole = psbi. Whereas the tetrafluoridoborate salt could not be crystallized for structure analysis [8b], a single crystalline material was isolated in the presence of hexafluoridophosphate. The structure analysis revealed a low anion content attributed to a partial deprotonation of the benzimidazole groups, a behavior, which is not uncommon in the coordination chemistry of imidazole-containing ligands [18, 19]. The following copper compounds were studied structurally:

$[Cu^{II}(msbi)_2Cl]Cl\cdot 2\,MeOH = [\mathbf{1}]Cl\cdot 2MeOH$
$[Cu^{II}(msbi)_2(MeOH)](BF_4)_2 = [\mathbf{2}](BF_4)_2$
$[Cu^{I}(mpsbi)_2](BF_4) = [\mathbf{3}](BF_4)$
$[Cu^{I}(psbi)_2][Cu^{I}(psbi)(psbi\text{-}H^+)](PF_6)\cdot CH_3CN = [\mathbf{4}][\mathbf{4'}](PF_6)\cdot CH_3CN$

Compounds also described are:
$[Cu^{I}(mpsbi)_2](PF_6) = [\mathbf{3}](PF_6)$
$[Cu^{I}(psbi)_2](PF_6) = [\mathbf{4}](PF_6)$
$[Cu^{I}(msbi)_2](PF_6) = [\mathbf{5}](PF_6)$

Results and Discussion

Ligand Synthesis and Structure

The preparations of msbi and psbi via 2-chloromethyl-*1H*-benzimidazole have been reported [8]. The ligand mpsbi was obtained similarly, or by reacting *N*-methyl-*o*-phenylenediamine with 2-phenylselenoacetic acid (Scheme 1) (see Experimental Section).

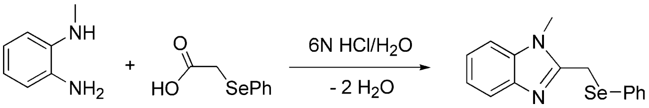

Scheme 1.

A structure determination of msbi (Table 1, Figure 1) revealed the expected non-planar conformation of the molecule in the crystal with typical bond parameters [20].

Copper(II) Complexes of msbi

Two different reactions of msbi with copper(II) precursors led to different crystalline materials. The reaction of msbi with $CuCl_2$ in methanol produced crystallographically characterized $[Cu(msbi)_2Cl]Cl\cdot 2MeOH$ (Figure 2, Table 1, Table 2), whereas the reaction with $Cu(BF_4)_2$ yielded $[Cu(msbi)_2(MeOH)](BF_4)_2$ (Figure 3, Table 1, Table 2).

Structurally, both copper(II) complex ions should be affected by ligand-caused effects, i.e. by the chelate bite within the five-membered metallacycle situation and by the considerable asymmetry between the hard, basic imidazole-N and the softer, assumedly [14] π-accepting selenoether-Se donor atoms.

The main feature striking in a comparative discussion of the two complexes is a mixed trigonal-bipyramidal/square-pyramidal structure (τ = 0.52 [21]) of the central cation $\mathbf{1}^+$ with the second and third row atoms chlorine and selenium in the equatorial plane, whereas the related $[Cu(msbi)_2(MeOH)](BF_4)_2$ exhibits a closer to square-pyramidal arrangement (Figure 4) with τ = 0.36 for the complex dication $\mathbf{2}^{2+}$. The parameter τ is defined as the difference between the basal *trans* angles, divided by 60°. A value of τ = 0 holds for the ideal square-pyramidal situation, a value of τ = 1 is calculated for the ideal trigonal-bipyramidal case [21]). Although the Se–Cu–Se angle in $\mathbf{1}^+$ is therefore decreased to about 137.75(2)° from 150.6(1)° in $\mathbf{2}^{2+}$, the Se···Se distance is beyond any interaction range at >4.5 Å. In both cases the Cu–N bond lengths are short and amount to about 1.94 Å, whereas the Cu–Se distances vary between 2.62 Å for $\mathbf{1}^+$ and ca. 2.54 Å for $\mathbf{2}^{2+}$.

The observed difference in structure for both $Cu^{II}(psbi)_2$ structures $\mathbf{1}^+$ and $\mathbf{2}^{2+}$ points to a sensitive situation with two

Table 1. Crystal and refinement data for ligand and complexes.

	msbi	[**1**](Cl)·2MeOH	[**2**](BF_4)$_2$	[**3**](BF_4)	[**4**][**4'**](PF_6)·CH_3CN
empirical formula	$C_9H_{10}N_2Se$	$C_{20}H_{28}Cl_2CuN_4O_2Se_2$	$C_{19}H_{24}B_2CuF_8N_4OSe_2$	$C_{30}H_{28}BCuF_4N_4Se_2$	$C_{58}H_{50}Cu_2F_6N_9PSe_4$
molar mass	225.15	648.82	719.52	752.83	1460.96
temperature /K	173(2)	293(2)	293(2)	293(2) K	173(2) K
wavelength /Å	0.71073	0.71073	0.71073	0.71073	0.71073
crystal system	orthorhombic	monoclinic	monoclinic	monoclinic	tetragonal
space group	*Pbca*	*C*2/*c*	*C*2/*c*	*C*2/*m*	*P*4/*n*
cell dimensions /Å	a = 8.7058(9) b = 9.7525(11) c = 21.747(2)	a = 17.516(4) b = 11.667(2) c = 12.566(3) β = 105.75(3)°	a = 21.4292(5) b = 17.6223(4) c = 16.4925(4) β = 121.096(1)°	a = 20.6470(7) b = 6.5126(3) c = 12.6499(6) β = 116.030(2)°	a = 13.6880(19) b = 13.6880(19) c = 15.174(3)
cell volume /Å^3	1846.4(3)	2471.6(9)	5333.1(2)	1528.44(11)	2843.0(8)
Z	8	4	8	2	2
calcd. density /Mg·m^{-3}	1.620	1.744	1.737	1.636	1.707
absorption coefficient /mm^{-1}	4.012	4.070	3.625	3.147	3.404
F(000)	896	1292	2808	748	1448
measured Θ region /°	1.87–26.99	1.06–29.00	1.02–28.28	3.28–24.69	1.085–29.00
index region	$-1 \le h \le 11$, $-1 \le k \le 12$, $-1 \le l \le 27$	$-22 \le h \le 23$, $-15 \le k \le 0$, $-17 \le l \le 0$	$-28 \le h \le 28$, $-23 \le k \le 23$, $-21 \le l \le 21$	$-24 \le h \le 24$, $-7 \le k \le 6$, $-14 \le l \le 14$	$-17 \le h \le 17$, $-17 \le k \le 17$, $-19 \le l \le 19$
no of reflections	2013	3281	6597	6867	3225
no of independent reflections	1441 [R_{int} = 0.0478]	2780 [R_{int} = 0.0269]	3268 [R_{int} = 0.0607]	2360 [R_{int} = 0.0564]	2383 [R_{int} = 0.1700]
absorption correction	PSI scan	PSI scan	empirical	numerical (HABITUS)	PSI scan
data/restraints/parameters	2013 / 0 / 117	3281 / 0 / 198	6597 / 0 / 334	6867/ 1 / 199	3225/0/186
goodness-of-fit on F^2	1.170	1.256	1.062	0.906	1.087
final R values [$I > 2\sigma(I)$]	R_1 = 0.0460, wR_2 = 0.0978	R_1 = 0.0336, wR_2 = 0.0727	R_1 = 0.0755, wR_2 = 0.1971	R_1 = 0.0422, wR_2 = 0.1156	R_1 = 0.0662, wR_2 = 0.1413
R values (all data)	R_1 = 0.0769, wR_2 = 0.1099	R_1 = 0.0460, wR_2 = 0.0771	R_1 = 0.0858, wR_2 = 0.2047	R_1 = 0.0513, wR_2 = 0.1245	R_1 = 0.0946, wR_2 = 0.1645
max/min electron density / e·Å^{-3}	0.473; –0.508	0.661; –0.562	4.002; –1.360	0.41; –0.27	0.164; –1.20

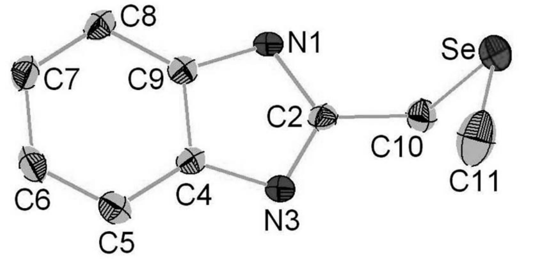

Figure 1. Molecular structure of msbi in the crystal [C10–Se 1.960(4) Å, Se–C11 1.934(5) Å, C10–Se–C11 97.1(2)°, C2–C10–Se–C11 66.0°].

strong Cu^{II}–N(imine) bonds, two weak Cu^{II}–Se(selenoether) interactions between a hard electrophile and two soft nucleophiles, and an additional donor with (Cl$^-$) or without (MeOH) charge. At 2.167(4) Å the Cu–O distance for bound methanol in $\mathbf{2}^{2+}$ is relatively short [22], the MeOH···FBF$_3$ hydrogen bonding at a shortest O···F distance of 2.99 Å lies in a typical range [8a, 23, 24]. The solvate molecules in [**1**](Cl)·2MeOH are connected to the non-coordinated chloride anion (Figure 2) by Cl···HO hydrogen bonds at Cl···O distance of 3.109(3) Å.

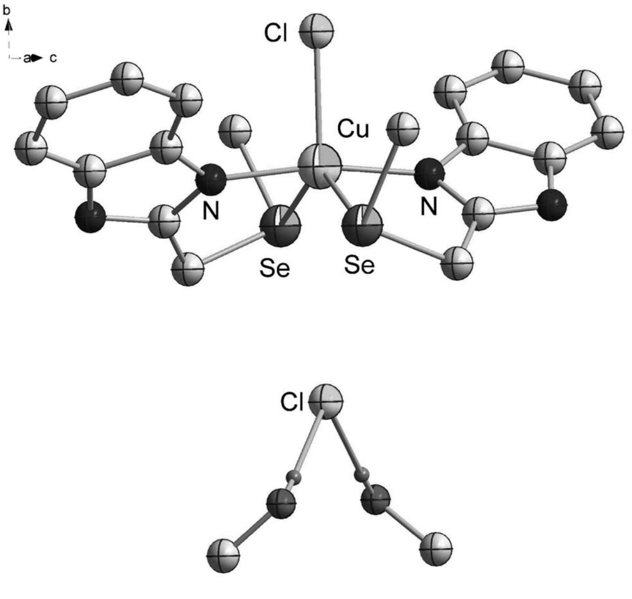

Figure 2. Molecular structures of cation $\mathbf{1}^+$ and solvated anion in the crystal of [**1**]Cl·2MeOH.

Slight differences between $\mathbf{1}^+$ and $\mathbf{2}^{2+}$ are also apparent from absorption and EPR spectra. Overall, the spectroscopy of the copper(II) compounds did not yield unusual results. Both systems exhibit standard EPR features at 110 K in frozen MeOH with $g_\perp$ = 2.063 (partially resolved hyperfine splitting), $A_\parallel$ = 11 mT for ^{63,65}Cu, and $g_\parallel$ = 2.25 ($\mathbf{1}^+$) or 2.32 ($\mathbf{2}^{2+}$), respectively. The absorption maxima of the weak (ε = 400 M^{-1}·cm^{-1}) d–d transitions lie at 760 nm ($\mathbf{1}^+$) or 690 nm ($\mathbf{2}^{2+}$), respectively.

Table 2. Selected bond parameters.

compound	Cu–N	Cu–Se	N–Cu–N	Se–Cu–Se	Se–Cu–N
[**1**]Cl•2MeOH	1.944(2)	2.6205(6)	169.17(12)	133.75(2)	82.60(6); 93.13(6)
[**2**](BF_4)$_2$	1.933(5)	2.532(1)	171.2(2)	150.60(4)	83.4(2); 94.8(2)
	1.947(5)	2.552(1)			82.7(2); 95.1(2)
[**3**](BF_4)	1.948(5)	2.632(1)	146.7(3)	110.91(6)	84.1(2);115.4(2)
[**4'**](PF_6)•CH_3CN	1.898(5)	2.849(1)	157.5(3)	78.23(4)	81.9(2); 116.4(2)

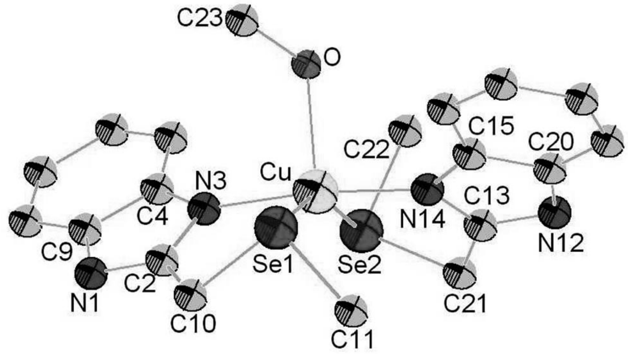

Figure 3. Molecular structure of $\mathbf{2}^{2+}$ in the crystal of [**2**](BF_4)$_2$.

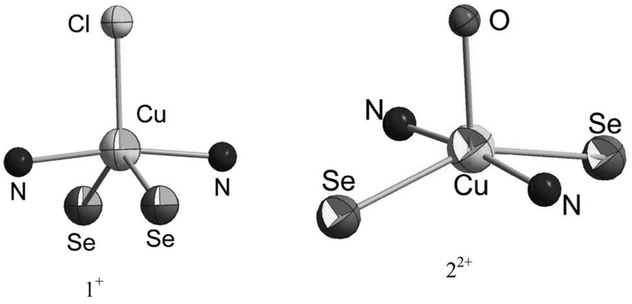

1^+ 2^{2+}

Figure 4. Coordination figures at the metal centers in the complex ions $\mathbf{1}^+$ (left) and $\mathbf{2}^{2+}$ (right).

Both the different charges and the different structural configurations can account for the spectroscopic variation. Whereas [**2**](BF_4)$_2$, which contains a labile methanol ligand, shows only irreversible reduction, the chloro complex [**1**]Cl_2 is reversibly reduced at +0.01 V versus ferrocenium/ferrocene in CH_2Cl_2/0.1 m Bu_4NPF_6. This lower number than for the oxidation of copper(I) complexes (see below) indicates the presence of charge compensating chloride.

Copper(I) Compounds

Although [**5**](PF_6) could be prepared and studied spectroscopically and electrochemically (cf. below), it could not be crystallized for X-ray structure analysis. We therefore modified the N,Se-chelate ligand by methylating the N1 position and using SePh as substituent to yield mpsbi, thus preventing N–H hydrogen bonding. Reaction of mpsbi with [Cu(CH_3CN)$_4$](PF_6) yielded [**3**](PF_6), reaction with Cu(BF_4)$_2$ resulted in copper reduction to yield crystallizing [**3**](BF_4). The reduction of copper(II) by Cu^I-coordinating organoelement compounds such as phosphines is not uncommon. The structural characterization of [**3**](BF_4) (Figure 5, Table 1, Table 2) shows a 2+2 coordination pattern [12] as for [Cu(mmb)$_2$](BF_4), however, with less pronounced straightening of the N–Cu–N angle at 146.7(3)° versus 169.8(1)° [6]. The selenium system thus approaches a more tetrahedral configuration than the related sulfur species. The remaining bond length and angle parameters are comparable with those of the Cu^I/mmb system [6] and with the copper(II)/Se species described above.

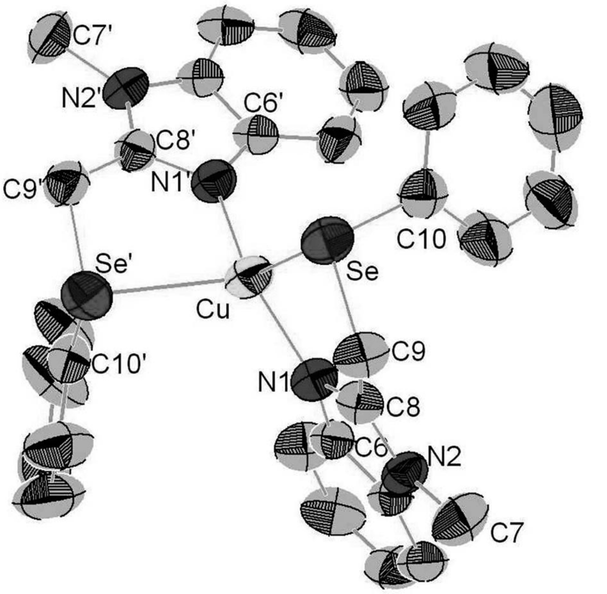

Figure 5. Molecular structure of cation $\mathbf{3}^+$ in the crystal of [**3**](BF_4).

To probe and confirm this S/Se effect we carried out DFT calculations for both species at comparable level. Table 3 shows that the agreement for the copper coordination environment is good, including particularly the differences in the N–Cu–N angles.

Due to the larger basis set used the DFT(ADF) optimized arrangement of [Cu(mmb)$_2$]$^+$ describes better the experimental geometry than the previously published calculations [6]. The substantial features of the experimental structure of [Cu(mpsbi)$_2$](BF_4) (Table 3) are confirmed by the calculations. In particular, the calculation reproduces nicely the experimentally observed lowering of the N–Cu–N angle on going from [Cu(mmb)$_2$]$^+$ to the related selenoether complex.

Table 3. Comparison of selected experimental and calculated bond lengths /Å and angles /° within [Cu(mpsbi)$_2$](BF$_4$) and [Cu(mmb)$_2$](BF$_4$).

	X = Se (L = mpsbi)		*X* = S (L = mmb)	
Bond length	exp. (this work)	calcd. (this work)	exp. [6]	calcd. (this work)
Cu–N(1)	1.948(5)	1.928	1.9199(18)	1.918
Cu–*X*	2.632(1)	2.636	2.6216(7)	2.702
X–C(9)	1.925(4)	1.982	1.801(3)	1.824
X–C(10)	1.914(5)	1.947	1.806(3)	1.826
Bond angle				
N(1)#1–Cu–N(1)	146.7(3)	146.3	169.75(11)	166.6
N(1)#1–Cu–*X*	115.35(15)	114.0	103.56(6)	106.9
N(1)–Cu–*X*	84.09(15)	86.0	82.47(6)	81.8
X–Cu–*X*#1	110.91(6)	109.1	109.33(3)	112.2
C(9)–*X*–Cu	90.47(12)	88.4	90.42(9)	89.7
C(10)–*X*–Cu	93.98(13)	96.1	93.7(1)	93.2
C(10)–*X*–C(9)	101.1(2)	100.3	100.7(1)	101.1
C(8)–N(1)–C(6)	104.5(5)	106.5	105.5(2)	106.4
C(8)–N(1)–Cu	123.6(4)	120.6	120.8(2)	120.6

Like for [Cu(mmb)$_2$]$^+$, the highest lying molecular orbital of the selenoether complex is mainly formed by a combination of *d* orbitals from the copper atom (61 %) with *p* orbitals of the chalcogen (18 %). The lowest lying unoccupied molecular orbital is composed from the π* orbital of the ligand with 11 % contribution from the selenium atom.

Using the psbi ligand, which previously yielded single crystalline Cu^{II} and Ag^I complexes [8b], we now managed to obtain not only a BF$_4^-$ salt [8b] but also a hexafluoridophosphate compound [Cu(psbi)$_2$](PF$_6$), which showed a fairly high stability versus oxidation. The single crystals isolated (see Experimental Section) were found to have the composition [Cu^I(psbi)$_2$][Cu^I(psbi)(psbi-H$^+$)](PF$_6$)·CH$_3$CN (Figure 6, Table 1, Table 2). This arrangement follows from the cation/anion ratio 2:1, which thus suggests a partially deprotonation of bound benzimidazole in psbi (3/4 occupancy of nitrogen bound hydrogen). Such deprotonations have been reported earlier [18, 19], they may be favored by the presence of the basic heterocycles and by advantageous crystal packing (Figure 7). Supporting this concept, the (averaged) Cu–N bond length is significantly shortened from about 1.94 Å in [**1**]$^+$, [**2**]$^{2+}$ and [**3**]$^+$ (Table 2) to 1.90 Å for [**4**][**4'**]$^+$. In correspondence, the Cu–Se bond length has increased from about 2.6 Å to 2.85 Å.

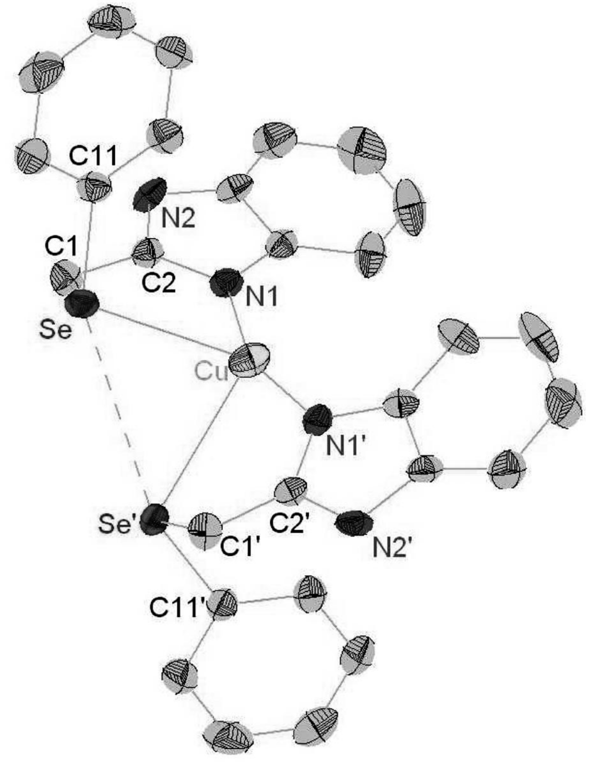

Figure 6. Molecular structure of averaged complexes in the crystal of [**4**][**4'**](PF$_6$)·CH$_3$CN.

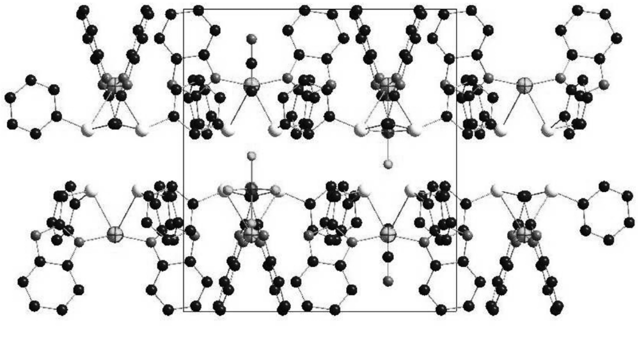

Figure 7. Packing in the unit cell of single crystalline [**4**][**4'**](PF$_6$)·CH$_3$CN.

An additional remarkable feature in [**4**][**4'**](PF$_6$) is the intramolecular Se···Se interaction at 3.6237(3) Å i.e. at lower distance than the sum of the van der Waals radii of ca. 3.8 Å [24]. The attraction is also reflected by the enormously diminished Se–Cu–Se angle of 78.23(4)° (Table 2).

The diamagnetic copper(I) compounds exhibit NMR spectra with rather small coordination induced shifts. Although [**4**](PF$_6$) in particular is rather resistant to oxidation, the copper(I) complexes are converted eventually in air to partly Se-oxygenated products [20].

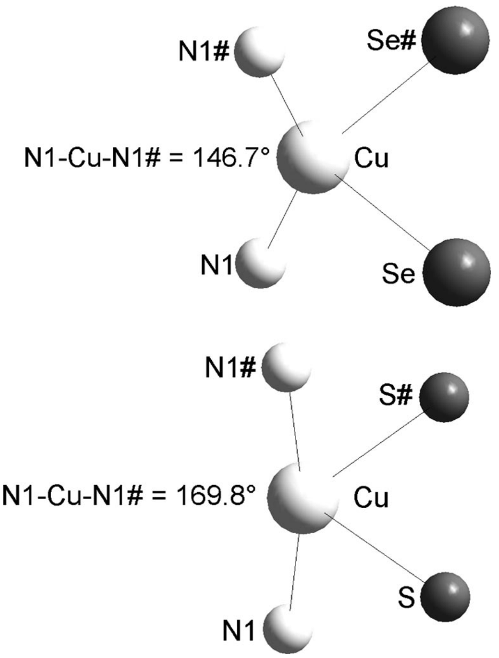

Figure 8. Coordination arrangement in $[Cu(mpsbi)_2]^+$ (top) and $[Cu(mmb)_2]^+$ (bottom).

The reversible oxidation of the copper(I) compounds in CH_2Cl_2/0.1 m Bu_4NPF_6 occurs at 0.29 V ($[\mathbf{5}]^+$), 0.38 V ($[\mathbf{4}]^+$) and 0.39 V $[\mathbf{3}]^+$ versus $Fc^{+/o}$, reflecting the easier oxidation for the Se-alkyl instead of the Se-aryl containing system. Nevertheless, the reversibility reflects a rather small reorganization barrier between the Cu^I and Cu^{II} states [6, 11], even with the selenoether donors present.

Conclusion

The metal coordination arrangements of the complex ions described herein illustrate some features distinguishing selenoether from thioether complexes, viz., the diminished N–Cu^I–N angle as a consequence of relatively stronger Cu^I–Se interaction and the possibility of Se···Se attraction. Remarkably, the replacement of the SR by the SeR function resulted in a *less* distorted-tetrahedral structure for copper(I) compounds.

The copper(II) systems are less remarkable, they show the tendency towards linear N–Cu^{II}–N angles (Table 2), even if the square-pyramidal coordination is not fully achieved. Additional ligands and the flexibility of the selenium donors allow for a considerable structural and spectroscopic (ESR, UV/Vis) variability. Nevertheless, cyclic voltammetric measurements still exhibit reversible electron transfer Cu^I/Cu^{II}, confirming the suitability also of selenoether ligands to tolerate both oxidation states.

Experimental Section

Instrumentation

^{1}H-NMR spectra were taken with a Bruker AC 250 and 400 spectrometers. EPR spectra were recorded with a Bruker ESP system. UV/Vis absorption spectra were obtained with a J & M Tidas spectrometer. Cyclic voltammetry was carried out in 0.1 M Bu_4NPF_6 solutions using a three-electrode configuration (glassy carbon working electrode, Pt counter electrode, Ag/AgCl reference) and a PAR 273 potentiostat and function generator. The ferrocenium/ferrocene (Fc^+/Fc) or decamethylferrocenium//decamethylferrocene couples served as internal reference.

Syntheses

2-Methylselenomethyl-*1H*-benzimidazole (msbi): A solution of dimethyl diselenide (0.60 g, 3.2 mmol) in THF (15 mL) was treated with an excess of 1 M $LiBHEt_3$ solution at –10 °C. Gas evolution, discoloring and turbidity accompany the reaction. After the gas evolution has ceased, EtOH (5 mL) was added for hydrolysis of excess $LiBHEt_3$. A suspension of 2-chloromethyl-*1H*-benzimidazole (1.2 g, 7.23 mmol) in EtOH (15 mL) was added dropwise and then stirred overnight. After removal of solvent the yellowish ligand is purified by column chromatography on silica 60 with an ethyl acetate/petroleum ether (1:1) mixture to yield 26 % of the product. Anal $C_9H_{10}N_2Se$ (225.15 g·mol^{-1}): calcd. C 47.86; H 4.48; N 12.44 %; found: C 48.01; H 4.61; N 12.17 %. **^{1}H NMR** (CD_3CN): δ = 2.04 (s, CH_3), 3.93 (s, CH_2), *J*(CH-^{77}Se 6.9 Hz); 7.15–7.25 (m, CH), 7.45–7.55 (m, CH). **^{13}C NMR** (CD_3CN): δ = 4.8 (CH_3), 19.7 (CH_2), *J*(^{13}C-^{77}Se 30 Hz); 115.7, 123.2, 139.3, 154.6. **^{77}Se NMR** (CD_3CN): δ = 155.

1-Methyl-2-phenylselenomethyl-*1H*-benzimidazole (mpsbi): A mixture of freshly distilled *N*-methyl-*o*-phenylenediamine (0.73 g, 6.0 mmol) and 2-phenylselenoacetic acid (1.31 g, 6.1 mmol) was heated under reflux for 20 h in half concentrated hydrochloric acid (25 mL). After removal of the excess hydrochloric acid under vacuum, the residue was suspended in H_2O (25 mL) and added slowly to cold concentrated ammonia (25 mL). Dark oil formed, which was extracted several times with dichloromethane. Drying with Na_2SO_4 and removal of CH_2Cl_2 yielded a brown solid, which was dissolved in ethyl acetate. After filtering the solution and adding a few drops of triethylamine, the mixture was purified by chromatography on a silica column (ethyl acetate/petroleum ether 80:20) to yield light brown oil, which solidified at 0 °C. Recrystallization from ethyl acetate yielded the light brownish product. Yield: 47 % (0.84 g). Anal $C_{15}H_{14}N_2Se$ (301.24 g·mol^{-1}): calcd. C 59.81; H 4.68; N 9.30 %; found: C 59.90; H 4.72; N 9.25 %. **^{1}H NMR** ($CDCl_3$): δ = 3.56 (s, CH_3), 4.31 (s, CH_2), 7.15–7.70 (m, CH). **^{13}C NMR** ($CDCl_3$): δ = 22.6 (CH_2), 30.5 (CH_3), 109.5, 119.9, 122.6, 123.1, 128.5, 129.6, 134.5, 134.6, 136.0, 143.3, 150.5. **^{77}Se NMR** ($CDCl_3$): δ = 937. The compound was alternatively obtained by the reaction of the corresponding 1-methyl-2-chloromethyl-*1H*-benzimidazole with $PhSe^-$ [8b].

$[Cu(msbi)_2Cl]Cl\cdot 2MeOH$ = $[\mathbf{1}](Cl)\cdot 2MeOH$: Msbi (100 mg, 0.44 mmol) and $CuCl_2$ (30 mg, 0.22 mmol) were dissolved in CH_3OH (10 mL) under gentle heating. Greenish crystals were obtained after slow cooling. Yield: 87 % (112 mg). Anal $C_{20}H_{28}Cl_2CuN_4O_2Se_2$ (648.82 g·mol^{-1}): calcd. C 37.02; H 4.13; N 8.64 %; found: C 36.10; H 4.35; N 8.73 %.

$[Cu(msbi)_2(MeOH)](BF_4)_2$ = $[\mathbf{2}](BF_4)_2$: Msbi (100 mg, 0.44 mmol) and $Cu(BF_4)_2$ (52 mg, 0.22 mmol) were dissolved in CH_3OH (2 mL). Green crystals were obtained after layering with diethyl ether (10 mL) and cooling to –18 °C. Yield: 35 % (56 mg). Anal $C_{19}H_{24}B_2CuF_8N_4OSe_2$ (719.50 g·mol^{-1}): calcd. C 31.72; H 3.36; N 7.79 %; found: C 31.45; H 3.62; N 7.60 %.

$[Cu(mpsbi)_2](PF_6)$ = $[\mathbf{3}](PF_6)$: The precursor compound $[Cu(CH_3CN)_4](PF_6)$ (50 mg, 0.134 mmol) and the ligand mpsbi

(81 mg, 0.268 mmol) were mixed under argon in CH_3CN (10 mL), stirred for 2 hours. Afterwards, the solvent was slowly removed to obtain the sensitive product. Yield: 72 mg (66 %). Anal $C_{30}H_{28}CuF_6N_4PSe_2$ (811.01 g·mol^{-1}): calcd. C 44.43; H 3.48; N 6.91 %; found: C 43.94; H 3.25; N 7.05 %. **^{1}H NMR** (CD_3CN): δ = 3.73 (s, CH_3), 4.42 (s, CH_2), J(CH_2–^{77}Se 6.9 Hz); 7.14–7.58 (m, CH). **^{13}C NMR** (CD_3CN): δ = 23.4 (CH_2), J(^{13}C-^{77}Se 30 Hz); 30.5 (CH_3), 110.7, 118.1, 123.1, 123.6, 128.2, 128.6, 129.2, 129.4, 129.6, 135.9, 155.2. **^{77}Se NMR** (CD_3CN): δ = 309.

[Cu(msbi)$_2$](PF$_6$) = [5](PF$_6$): The precursor $[Cu(CH_3CN)_4](PF_6)$ (50 mg, 0.134 mmol) and the ligand msbi (60 mg, 0.268 mmol) were stirred in CH_3CN (10 mL) for 2 hours. Afterwards, the solvent was slowly removed to obtain the very sensitive product. Yield: 68 mg (72 %). Anal $C_{18}H_{20}CuF_6N_4PSe_2$ (658.81 g·mol^{-1}): calcd. C 32.82; H 3.06; N 8.51 %; found: C 32.78; H 2.97; N 9.10 %. **^{1}H NMR** (CD_3CN): δ = 2.11 (s, CH_3), 4.05 (s, CH_2); 7.28–7.62 (m, CH). **^{13}C NMR** (CD_3CN): δ = 6.3 (CH_3), 21.3 (CH_2), 30.5 (CH_3), 115.1, 123.1, 129.7, 154.8.

[Cu(mpsbi)$_2$](BF$_4$) = [3](BF$_4$): A solution of mpsbi (83 mg, 0.28 mmol) in MeOH (3 mL) was treated with a solution of $Cu(BF_4)_2·6H_2O$ (48 mg, 0.14 mmol) in MeOH (3 mL). The dark-green solution was stirred for one day. Afterwards, the solvent volume was reduced to 50 % and a green solid precipitated by cooling to 4 °C. Redissolving in dry MeOH and keeping at 4 °C produced colorless crystals (rods) suitable for X-ray diffraction. Yield: 12 mg (11 %). **^{1}H NMR** ($CDCl_3$): δ = 3.71 (s, CH_3), 4.45 (s, CH_2), 7.15–7.70 (m, CH).

[Cu(psbi)$_2$](PF$_6$) = [4](PF$_6$): The precursor compound $[Cu(CH_3CN)_4](PF_6)$ (50 mg, 0.134 mmol) and the ligand psbi (77 mg, 0.268 mmol) were mixed under argon in CH_3CN (10 mL), stirred for 2 hours, and the solvent was slowly removed to yield 87 mg (83 %) of the product. Anal $C_{28}H_{24}CuF_6N_4PSe_2$ (782.95 g·mol^{-1}): calcd. C 42.95; H 3.09; N 7.16 %; found: C 42.56; H 3.45; N 6.86 %. **^{1}H NMR** (CD_3CN): δ = 4.39 (s, CH_2), 7.18–7.60 (m, CH). **^{13}C NMR** (CD_3CN): δ = 26.0, 117.8, 124.4, 129.0, 129.6, 130.0, 133.5, 163.5, 186.0. Crystallization at –18 °C of an acetonitrile solution produced single crystals of $[Cu^I(psbi)_2][Cu^I(psbi)(psbi\text{-}H^+)](PF_6)·CH_3CN$ = [**4**][**4'**]$(PF_6)·CH_3CN$. Anal. $C_{58}H_{50}Cu_2F_6N_9PSe_4$ (1462.901 g·mol^{-1}): calcd. C 47.68; H 3.45; N 8.63 %, found: C 47.58; H 3.54; N 8.66 %.

Crystal Structure Determination

Colorless single crystals of [**3**](BF_4) were obtained from a methanol solution at 4 °C. Green single crystals of [**2**]$(BF_4)_2$ were grown by slow diffusion of diethyl ether into a methanol solution. Data for both crystals were collected at 293 K with a NONIUS Kappa CCD diffractometer. Green single crystals of [**1**]Cl·2MeOH were obtained by slow evaporation from a saturated methanol solution, single crystals of [**4**][**4'**]$(PF_6)·CH_3CN$ were obtained from a concentrated acetonitrile solution, and single crystals of msbi were grown from an ethyl acetate/petroleum ether (1:1) mixture by slow evaporation at room temperature. Data collection for these crystals was performed at 173 K (msbi, [**4**][**4'**]$(PF_6)·CH_3CN$) and 293 K ([1]Cl·2 MeOH) with a Siemens P4 diffractometer employing the ω-2θ scan technique. The structures were solved by direct methods using the SHELXTL package [25], and refinement was carried out with SHELXL97 employing full-matrix least-squares methods on F^2 with $F_o^2 \geq 2\sigma(F_o^2)$. All non-hydrogen atoms were treated anisotropically; hydrogen atoms were included by using appropriate riding models. Additional crystallographic information is given in Table 1.

Crystallographic data have been deposited with the Cambridge Crystallographic Data Centre, CCDC-722404, -722405, -722406, -722407, and -722408. Copies of the information may be obtained free of charge from: The Director, CCDC, 12 Union Road, Cambridge CB2 1EZ, UK (Fax: +44-1223-336-033; E-Mail: deposit@ccdc.cam.ac.uk; www: http://www.ccdc.cam.ac.uk).

DFT Calculations

Ground state electronic structure calculations of the complex ions $[Cu(mmb)_2]^+$ and $[Cu(mpsbi)_2]^+$ (see Figure 8) were performed by the density-functional theory (DFT) method using ADF2007.1 [26–28]. Slater type orbital (STO) basis sets of triple-ζ quality with two polarization functions for sulfur, selenium, and copper and triple-ζ quality with one polarization function for the other atoms were employed. The inner shells were represented by the frozen core approximation (1s for C, N, 2p for S, 3p for Se and 1s–2p for Cu were kept frozen). The following density functionalisms were used within ADF: The local density approximation (LDA) with VWN parameterization of electron gas data or the functional including *Becke*'s gradient correction [29] to the local exchange expression in conjunction with *Perdew*'s gradient correction [30] to the LDA expression (ADF/BP). The scalar relativistic (SR) zero order regular approximation (ZORA) was used within this study. Geometry optimizations were done without any symmetry constraints.

Acknowledgement

This work was supported by the *Deutsche Forschungsgemeinschaft* (SFB 706), the *Fonds der Chemischen Industrie*, the EU (COST D35), the *Grant Agency of the Academy of Sciences of the Czech Republic* (KAN 100400702) and the *Ministry of Education of the Czech Republic* (Grant COST OC 139).

References

[1] a) A. Panda, S. C. Menon, H. B. Singh, C. P. Morley, R. Bachman, T. M. Cocker, R. J. Butcher, *Eur. J. Inorg. Chem.* **2005**, 1114; b) S. G. Murray, F. R. Hartley, *Chem. Rev.* **1981**, *81*, 365.

[2] a) S. Dey, L. B. Kumbhare, V. K. Jain, T. Schurr, W. Kaim, A. Klein, F. Belaj, *Eur. J. Inorg. Chem.* **2004**, 4510; b) S. Dey, V. K. Jain, A. Knödler, A. Klein, W. Kaim, S. Zalis, *Inorg. Chem.* **2002**, *41*, 2864; c) S. Dey, V. K. Jain, S. Chaudhury, A. Knoedler, F. Lissner, W. Kaim, *J. Chem. Soc., Dalton Trans.* **2001**, 723.

[3] a) C. Jacob, G. I. Giles, N. M. Giles, H. Sies, *Angew. Chem.* **2003**, *115*, 4890; *Angew. Chem. Int. Ed.* **2003**, *42*, 4742; b) W.-W. du Mont, G. Mugesh, C. Wismach, P. G. Jones, *Angew. Chem.* **2001**, *113*, 2547; *Angew. Chem. Int. Ed.* **2001**, *40*, 2486.

[4] H. Engelberg-Kulka, R. Schoulaker-Schwarz, *Trends Biochem. Sci.* **1988**, *13*, 419.

[5] a) G. Roelfes, D. Hilvert, *Angew. Chem.* **2003**, *115*, 2377; *Angew. Chem. Int. Ed.* **2003**, *42*, 2275; b) G. N. Schrauzer, *Adv. Food Nutr. Res.* **2003**, *47*, 73; c) S. M. Berry, M. Ralle, D. W. Low, N. J. Blackburn, Y. Lu, *J. Am. Chem. Soc.* **2003**, *125*, 8760.

[6] M. Albrecht, K. Hübler, S. Zalis, W. Kaim, *Inorg. Chem.* **2000**, *39*, 4731.

[7] a) J. Rall, E. Waldhör, B. Schwederski, M. Schwach, S. Kohlmann, W. Kaim, in *Bioinorganic Chemistry: Transition Metals in Biology and their Coordination Chemistry*, (Ed.: A. X. Trautwein), VCH, Weinheim, Germany, **1997**, p 476; b) M. Albrecht, K. Hübler, T. Scheiring, W. Kaim, *Inorg. Chim. Acta* **1999**, *287*, 204; c) W. Kaim, M. Wanner, A. Knödler, S. Zalis, *Inorg. Chim. Acta* **2002**, *337*, 163.

[8] a) M. Leboschka, M. Sieger, M. Niemeyer, S. Záliš, W. Kaim, *Z. Anorg. Allg. Chem.* **2008**, *634*, 2343; b) M. Leboschka, M. Sieger, B. Sarkar, M. Niemeyer, T. Schurr, J. Fiedler, S. Záliš, W. Kaim, *Z. Anorg. Allg. Chem.* **2009**, *635*, 1001.

[9] J. Rall, M. Wanner, M. Albrecht, F. M. Hornung, W. Kaim, *Chem. Eur. J.* **1999**, *5*, 2802.

[10] a) M. Mure, *Acc. Chem. Res.* **2004**, *37*, 131; b) R. Medda, A. Padiglia, A. Bellelli, J. Z. Pedersen, A. Finazzi Agro, G. Floris, *FEBS Lett.* **1999**, *453*, 1; c) R. Medda, A. Mura, S. Longu, R. Anedda, A. Padiglia, M. Casu, G. Floris, *Biochimie* **2006**, *88*, 827.

[11] a) D. B. Rorabacher, *Chem. Rev.* **2004**, *104*, 651; b) S. Torelli, C. Belle, C. Philouze, J.-L. Pierre, W. Rammal, E. Saint-Aman, *Eur. J. Inorg. Chem.* **2003**, 2452.

[12] a) S. Alvarez, P. Alemany, D. Casanova, J. Cirera, M. Llunell, D. Avnir, *Coord. Chem. Rev.* **2005**, *249*, 1693; b) I. Persson, K. B. Nilsson, *Inorg. Chem.* **2006**, *45*, 7428; c) S. Ekici, M. Nieger, R. Glaum, E. Niecke, *Angew. Chem.* **2003**, *115*, 451; *Angew. Chem. Int. Ed.* **2003**, *42*, 435.

[13] a) M. Afzaal, D. J. Crouch, P. O'Brien, J. Raftery, P. J. Skabara, A. J. P. White, D. J. Williams, *J. Mater. Chem.* **2004**, *14*, 233; b) D. L. Castro, S. G. Bailey, R. P. Rafaelle, K. K. Banger, A. F. Hepp, *Chem. Mater.* **2003**, *15*, 3142; c) J. J. Vittal, M. T. Ng, *Acc. Chem. Res.* **2006**, *39*, 869.

[14] a) H.-B. Kraatz, H. Jacobsen, T. Ziegler, P. M. Boorman, *Organometallics* **1993**, *12*, 76; b) W. Kaim, *J. Biol. Inorg. Chem.* **2007**, *12*, S121.

[15] a) A. V. Davis, T. O'Halloran, *Nature Chem. Biol.* **2008**, *4*, 148; b) C. Belle, W. Rammal, J.-L. Pierre, *J. Inorg. Biochem.* **2005**, *99*, 1929.

[16] S. T. Prigge, B. A. Eipper, R. E. Mains, L. M. Amzel, *Science* **2004**, *304*, 864.

[17] a) L. Zhou, D. Powell, K. M. Nicholas, *Inorg. Chem.* **2006**, *45*, 3840; b) L. Q. Hatcher, D.-H. Lee, M. A. Vance, A. E. Milligan, R. Sarangi, K. O. Hodgson, B. Hedman, E. I. Solomon, K. D. Karlin, *Inorg. Chem.* **2006**, *45*, 10055; c) N. W. Aboelella, B. F. Gherman, L. M. R. Hill, J. T. York, N. Holm, V. G. Young Jr., C. J. Cramer, W. B. Tolman, *J. Am. Chem. Soc.* **2006**, *128*, 3445.

[18] C.-L. Chen, Q. Zhang, J.-H. Yao, J.-Y. Zhang, B.-S. Kang, C.-Y. Su, *Inorg. Chim. Acta* **2008**, *361*, 2934.

[19] a) C.-Y. Su, A. M. Goforth, M. D. Smith, P. J. Pellechia, H.-C. zur Loye, *J. Am. Chem. Soc.* **2004**, *126*, 3576; b) C.-L. Chen, H.-Y. Tan, J.-H. Yao, Y.-Q. Wan, C.-Y. Su, *Inorg. Chem.* **2005**, *44*, 8510; c) X.-L. Zhang, S.-R. Zheng, Y.-R. Liu, X.-L. Zheng, C.-Y. Su, *Acta Crystallogr., Sect. C* **2005**, *61*, 533; d) S.-R. Zheng, Y.-P. Cai, X.-L. Zhang, C.-Y. Su, *Acta Crystallogr., Sect. C* **2005**, *61*, 642.

[20] M. Leboschka, Ph. D. Thesis, University of Stuttgart, **2009**.

[21] a) A. W. Addison, T. N. Rao, J. Reedijk, J. van Rijn, G. C. Verschoor, *J. Chem. Soc., Dalton Trans.* **1984**, 1349; b) A. Schmuck, K. Seppelt, *Chem. Ber.* **1989**, *122*, 803.

[22] a) G. van Albada, W. Smeets, A. Spek, J. Reedijk, *J. Chem. Crystallogr.* **1998**, *28*, 427; b) O. Nobuo, M. Yasunori, O. Mamiko, *Acta Crystallogr., Sect. C* **2004**, *60*, 345.

[23] R. W. M. Ten Hoedt, W. L. Driessen, G. C. Verschoor, *Acta Crystallogr., Sect. C* **1983**, *39*, 71.

[24] J. E. Huheey, E. A. Keiter, R. L. Keiter, *Inorganic Chemistry*, 4th ed., Harper Collins, New York, **1993**, p 292.

[25] a) G. M. Sheldrick, *Program for Crystal Structure Solution and Refinement*, Universität Göttingen, **1997**; b) G. M. Sheldrick, *SHELXTL*, version 5.10; Bruker AXS Inc., Madison, Wisconsin, **1998**.

[26] a) G. te Velde, F. M. Bickelhaupt, S. J. A. van Gisbergen, C. Fonseca Guerra, E. J. Baerends, J. G. Snijders, T. Ziegler, *J. Comput. Chem.* **2001**, *22*, 931; b) ADF2007.01, SCM, Theoretical Chemistry, Vrije Universiteit, Amsterdam, The Netherlands, http://www.scm.com

[27] C. Fonseca Guerra, J. G. Snijders, G. te Velde, E. J. Baerends, *Theor. Chem. Acc.* **1998**, *99*, 391.

[28] S. J. A. van Gisbergen, J. G. Snijders, E. J. Baerends, *Comput. Phys. Commun.* **1999**, *118*, 119.

[29] A. D. Becke, *Phys. Rev. A* **1988**, *38*, 3098.

[30] J. P. Perdew, *Phys. Rev. A* **1986**, *33*, 8822.

Received: May 11, 2009